Observer-based MPC of an Axial Dispersion Tubular Reactor: Addressing Recycle Delays through Transport PDEs

Behrad Moadeli and Stevan Dubljevic[1]

***Abstract*— The model predictive control of an axial dispersion tubular reactor equipped with a recycle stream is presented. The intrinsic time delay imposed by the recycle stream, an often overlooked aspect in chemical engineering process control studies, is modeled as a transport PDE, leading to a boundary-controlled system of coupled parabolic and hyperbolic PDEs under Danckwerts boundary conditions, suitable for this reactor type. Considering the digital nature of controllers, a discrete-time linear model predictive controller is designed to stabilize the system, coupled with a Luenberger state estimator to address the controller's limited access to the system's full state. The need for model reduction through spatial approximation is eliminated by following a late lumping approach, while utilizing Caley-Tustin time discretization method to preserve the continous-time system's characteristics. The controller's effectiveness is demonstrated through numerical simulations, showcasing its capability to stabilize an unstable system while adhering to input constraints, having access merely to output measurements.**

I. Introduction

Many processes in the chemical and petrochemical sectors involve states that evolve over space and time, commonly represented by partial differential equations (PDEs) as distributed parameter systems (DPS) [1]. The infinite-dimensional nature of DPSs presents specific challenges in control and estimation, making this a prominent area of research. Two main methods are often applied to control DPSs: *Early Lumping* and *Late Lumping*. Early Lumping reduces the system to a finite-dimensional approximation through spatial discretization early in the modeling stage, allowing for the application of standard control techniques [2]. However, this method can lead to inaccuracies due to mismatches between the reduced model and the original system dynamics [3]. Late Lumping, by contrast, preserves the system's infinite-dimensional structure until the final stages of controller implementation, resulting in a control approach that is more complex but achieves greater fidelity to the original dynamics.

A range of studies in chemical engineering have applied the late lumping method to control infinite-dimensional systems, specifically targeting convection-reaction processes governed by first-o rder hyperbolic PDEs and diffusion-convection-reaction processes described by second-order parabolic PDEs. In [4], the robust control of first-order hyperbolic PDEs is explored, demonstrating the stabilization of a plug flow reactor system using a distributed input. A boundary feedback stabilization approach using the backstepping method is presented in [5] for a comparable system of first-order hyperbolic PDEs. The work in [6] introduces a state feedback regulator design for a countercurrent heat exchanger system, providing another example of a chemical engineering DPS governed by first-order hyperbolic PDEs, distinct from tubular reaction systems. Highlighting the role of dispersion in axial dispersion tubular reactors, [7] examines the robust control of diffusion-convection-reaction systems governed by second-order parabolic PDEs. In [8], a late-lumping approach is employed to develop a low-dimensional predictive controller for a diffusion-convection-reaction system, utilizing modal decomposition to capture the system's dominant modes. A similar method is applied in [9] to design an observer-based model predictive controller (MPC) for an axial dispersion tubular reactor, accounting for the impact of recycle streams, a common feature in industrial chemical reactors. Different aspects of state reconstruction for DPSs are addressed in several works where the design of a discrete-time Luenberger observer is adressed for the class of DPSs, where no spatial discretization is required; a key feature of the late lumping approach [10]–[13].

In addition to dynamic systems distributed over space, dynamic systems that exhibit time delays are also classified as DPSs [14]. In the field of control theory for infinite-dimensional systems, delay systems are either represented as delay differential equations (DDEs) or as transport PDEs, with the latter being advantageous in more complex scenarios, e.g. in the presence of spatial dynamics [15]. When it comes to chemical engineering applications of control theory, delays are often introduced as the result of inout or output delays, while state delays are less frequently addressed in the literature; most probably since not many applications in this field can be described by state delays, in contrast with other domains of control theory, such as signal processing or mechanical systems. Input/output delays are generally handled by introducing a transportation lag block at either the input or output of the system, leading to a cascade PDE system [16]–[18]. In one of the few studies addressing state delays in this area, [19] investigates a delayed-state distributed parameter system where a full-state and output feedback regulator is designed for a heat exchanger system. Here, the state delay arises from the time taken for a stream to exit one pass of the heat exchanger and enter the next. Similarly, in [20], a tubular reactor system is considered, where state delay is introduced by the recycle delay in the system, without

[1]Behrad Moadeli and Stevan Dubljevic are with the Department of Chemical and Materials Engineering, University of Alberta, Edmonton, AB, Canada T6G 1H9 moadeli@ualberta.ca, stevan.dubljevic@ualberta.ca

Funding provided by the Natural Sciences and Engineering Research Council of Canada—NSERC (RGPIN-2022-03486).

accounting for the diffusion term along the reactor. Even in [9], where a recycle stream is incorporated for a distributed diffusion-convection-reaction system, the recycle is assumed to be instantaneous—an assumption that creates a gap in the literature on diffusion-convection-reaction systems with recycle streams that impose state delay.

In this work, an axial dispersion tubular reactor equipped with recycle is addressed as a diffusion-convection-reaction DPS. First, the reactor is modeled by a second order parabolic PDE, where the recycle stream poses a state delay, resulting in a first order hyperbolic transport PDE. Therefore, a system of coupled hyperbolic and parabolic PDEs is obtained to describe the infinite-dimensional model of the plant. The resolvent operator of the system is then obtained in am exact closed form, omitting the need for spatial discretization following the late lumping approach. The continous-time system is then discrtetized to enable the implementation of MPC as a digital controller. This is done using Caley-Tustin time discretization technique, i.e. a Crank-Nicolson type of discretization that preserves the conservative characteristics of the continuous system, mitigating the need for model reduction [21], [22]. An infinite-dimensional Luenberger observer is also designed to reconstruct the states of the system, addressing the controller's limited access to system's full-state. As a result, through numerical simulations, the observer-based output feedback MPC is shown to successfully stabilize a system while adhering to input constraints, despite the original system being unstable.

II. Continuous-time Model Representation

Fig. 1 illustrates a chemical process, i.e. a first-order irreversible reaction within an axial dispersion tubular reactor [23]. The reactor is equipped with a recycle mechanism, allowing a portion of the product stream to re-enter the reactor, increasing the conversion of the substrate. Utilizing first-principle modeling through relevant mass balance relations on an infinitesimally thin disk element along the longitudinal axis of the reactor, the dynamics describing the concentration within the system results in a second-order parabolic PDE, a common class of equations used to characterize diffusion-convection-reaction systems [24].

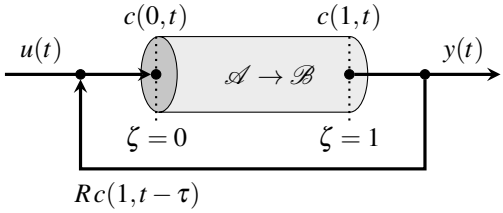

Fig. 1. Axial tubular reactor with recycle stream.

In an attempt to make the model more realistic for common axial dispersion tubular reactors in chemical industry, Dankwerts boundary conditions are chosen as they are known to be suitable for this purpose by accounting for deviations from perfect mixing and piston flow, assuming negligible transport lags in connecting lines [25]. The delayed state resulting from the recycled portion of the flow, occurring τ seconds back in time, is applied at the inlet boundary condition. The governing equation is given by the PDE represented by (1), subject to the abovementioned boundary conditions in (2).

$$\dot{c}(\zeta,t) = D\partial_{\zeta\zeta}c(\zeta,t) - v\partial_{\zeta}c(\zeta,t) + k_r c(\zeta,t) \tag{1}$$

$$\begin{cases} D\partial_{\zeta}c(0,t) - vc(0,t) = -v\left[Rc(1,t-\tau) + (1-R)u(t)\right] \\ \partial_{\zeta}c(1,t) = 0 \\ y(t) = c(1,t) \end{cases} \tag{2}$$

Here, $c(\zeta,t)$ is the concentration of the product along the reactor, representing the state of the system. The physical parameters D, v, k_r, R, and τ represent the diffusion coefficient, flow velocity along the reactor, reaction constant, recycle ratio, and residence time of the recycle flow, respectively. The coordinate system in space and time is represented by ζ and t, where $\zeta \in [0,1]$ and $t \in [0,\infty)$.

An interesting approach to address delays where the problem involves other forms of PDEs is to reformulate the problem such that the notion of delay is replaced with an alternative transport PDE [15]. Therefore, the state variable $c(\zeta,t)$ is replaced with a new state variable $\underline{x}(\zeta,t) \equiv [x_1(\zeta,t), x_2(\zeta,t)]^T$ as a vector of functions, where $x_1(\zeta,t)$ represents the concentration within the reactor—analogous to $c(\zeta,t)$—and $x_2(\zeta,t)$ is the new state variable for the concentration along the recycle stream. The delay is thus modeled as a pure transport process rather than being present in the argument of the state at the boundary—i.e. $c(1,t-\tau)$—making all state variables expressed explicitly at a specific time instance t, resulting in the standard state-space form for a given infinite-dimensional linear time-invariant (LTI) system given in (3).

$$\begin{aligned} \dot{\underline{x}}(\zeta,t) &= \mathfrak{A}\underline{x}(\zeta,t) + \mathfrak{B}u(t) \\ y(t) &= \mathfrak{C}\underline{x}(\zeta,t) \end{aligned} \tag{3}$$

Here, $\mathfrak{A}$ is a linear operator $\mathscr{L}(X)$ acting on a Hilbert space $X : L^2[0,1] \times L^2[0,1]$ and $\underline{x}(\zeta,t)$, as defined previously, is the vector of functions describing the states of the system. The operator $\mathfrak{A}$ and its domain are defined in (4). Also, $\mathfrak{B}$ is a linear operator that maps the scalar input from input-space onto the state space, as defined in (5). Finally, the output operator $\mathfrak{C}$ is defined in (6), where it maps the state to the output $y(t)$, which is the concentration at the reactor outlet according to (2).

$$\mathfrak{A} \equiv \begin{bmatrix} D\partial_{\zeta\zeta} - v\partial_\zeta + k_r & 0 \\ 0 & \frac{1}{\tau}\partial_\zeta \end{bmatrix}$$

$$\begin{aligned} \mathscr{D}(\mathfrak{A}) = \Big\{ & \underline{x}(\zeta) = [x_1(\zeta), x_2(\zeta)]^T \in X : \\ & \underline{x}(\zeta), \partial_\zeta \underline{x}(\zeta), \partial_{\zeta\zeta}\underline{x}(\zeta) \quad \text{a.c.}, \\ & D\partial_\zeta x_1(0) - v x_1(0) = -vR x_2(0), \\ & \partial_\zeta x_1(1) = 0, x_1(1) = x_2(1) \Big\} \end{aligned} \tag{4}$$

$$\mathfrak{B} \equiv \begin{bmatrix} \delta(\zeta) \\ 0 \end{bmatrix} \cdot (1-R)v \tag{5}$$

$$\mathfrak{C} \equiv \begin{bmatrix} \delta(\zeta - 1) & 0 \end{bmatrix} \tag{6}$$

with $\delta(\zeta)$ being dirac delta function. The system's spectrum can now be obtained by solving the eigenvalue problem for the system generator $\mathfrak{A}$. To do this, the characteristics equation of the system needs to be obtained by solving the equation $det(\mathfrak{A} - \lambda_i\ I) = 0$ for λ_i, where $\lambda_i \in \mathbb{C}$ is the i^{th} eigenvalue of the system and I is the identity operator. Attempts to analytically solve this equation will fail; therefore, it is solved numerically given the parameters in Table I. The eigenvalue distribution is given in Figure 2 in the complex plane. This suggests that the open-loop system is unstable, as there are eigenvalues with positive real parts.

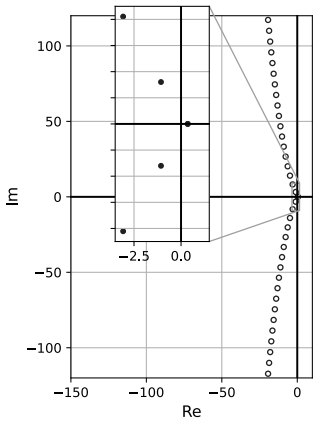

Fig. 2. Eigenvalues of operator $\mathfrak{A}$.

TABLE I
PHYSICAL PARAMETERS FOR THE SYSTEM

Parameter	Symbol	Value	Unit
Diffusivity	D	2×10^{-5}	m^2/s
Velocity	v	0.01	m/s
Reaction Constant	k_r	1.5	s^{-1}
Recycle Residence Time	τ	80	s
Recycle Ratio	R	0.3	–

It is necessary to obtain the adjoint system operators $\mathfrak{A}^*$ and $\mathfrak{B}^*$ in order to derive the resolvent operator of the system, which is later utilized in performing the Caley-Tustin time discretization. The derivation of the adjoint system operators is provided in Appendix A, followed by the derivation of an exact closed-form representation for the resolvent operator detailed in Appendix B.

III. CALEY-TUSTIN TIME DISCRETIZATION

Having access to the resolvent operators of the original and the adjoint system, the Caley-Tustin time-discretization may be utilized to map the continuous-time setting to the discrete-time setting without losing crucial dynamical properties of the system, such as stability and controllability. This Crank-Nicolson type of discretization is also known as the lowest order symplectic integrator in Gauss quadrature-based Runge-Kutta methods [26]. Considering Δt as the sampling time, and assuming a piecewise constant input within time intervals (a.k.a. zero-order hold), the discrete-time representation $\underline{x}(\zeta,k) = \mathfrak{A}_d\underline{x}(\zeta,k-1) + \mathfrak{B}_d u(k)$ is obtained, with discrete-time operators $\mathfrak{A}_d$ and $\mathfrak{B}_d$ defined in (7), where $\alpha = 2/\Delta t$. As required for systems with nonself-adjoint generators, the adjoint discrete-time operators $\mathfrak{A}_d^*$ and $\mathfrak{B}_d^*$ are also obtained in a similar manner.

$$\begin{bmatrix} \mathfrak{A}_d & \mathfrak{B}_d \\ \mathfrak{C}_d & \mathfrak{D}_d \end{bmatrix} = \begin{bmatrix} -I + 2\alpha\mathfrak{R}(\alpha,\mathfrak{A}) & \sqrt{2\alpha}\mathfrak{R}(\alpha,\mathfrak{A})\mathfrak{B} \\ \sqrt{2\alpha}\mathfrak{C}\mathfrak{R}(\alpha,\mathfrak{A}) & \mathfrak{C}\mathfrak{R}(\alpha,\mathfrak{A})\mathfrak{B} \end{bmatrix} \tag{7}$$

IV. OBSERVER DESIGN

One important issue of DPSs is the limitted access to the states of the infinite-dimensional system as the state is distributed over the entire domain and performing infinite measurements is never feasible. Therefore, an observer is required to estimate the states of the system based on the available measurements. To address this issue, a Luenberger observer is designed to reconstruct the states of the system based on the output measurements. First, the consinuous-time observer design is considered; followed by the design of the discrete-time observer.

A. Continuous-Time Observer Design

For the purpose of state recunstruction of a diffusion-convection-reaction system, where the feedforward term $\mathfrak{D}$ is generally absent, the continuous-time observer dynamics are given by (8).

$$\begin{aligned} \dot{\underline{\hat{x}}}(\zeta,t) &= \mathfrak{A}\underline{\hat{x}}(\zeta,t) + \mathfrak{B}u(t) + \mathfrak{L}_c[y(t) - \hat{y}(t)] \\ \hat{y}(t) &= \mathfrak{C}\underline{\hat{x}}(\zeta,t) \end{aligned} \tag{8}$$

where $\underline{\hat{x}}(\zeta,t)$ is the reconstructed state of the original system and $\mathfrak{L}_c$ is the continuous-time observer gain. By subtracting the observer dynamics from the original system dynamics, the error dynamics $e(\zeta,t)$ are obtained as shown in (9).

$$\dot{e}(\zeta,t) = (\mathfrak{A} - \mathfrak{L}_c\mathfrak{C})e(\zeta,t) \equiv \mathfrak{A}_o e(\zeta,t) \tag{9}$$

The goal is to design the observer gain $\mathfrak{L}_c$ such that the error dynamics are exponentially stable, i.e. $\max\{\text{Re}(\lambda_o)\} < 0$ where $\{\lambda_o\}$ is the set of eigenvalues of the error dynamics operator $\mathfrak{A}_o$. Three different forms of the observer gain are considered as spatial functions $\mathfrak{L}_c = f(\zeta, l_{obs})$ with the effect of the scalar coefficient l_{obs} on $\max\{\text{Re}(\lambda_o)\}$ shown in Fig. 3.

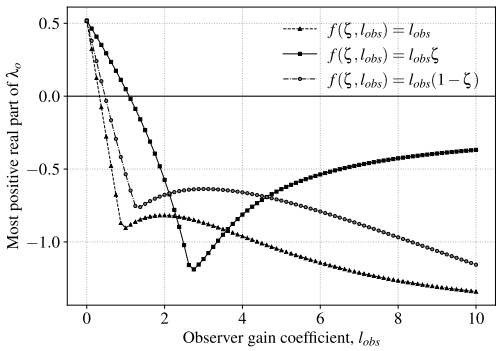

Fig. 3. The effect of various observer gains $\mathfrak{L}_c = f(\zeta, l_{obs})$ on the eigenvalues of state reconstruction error dynamics λ_o.

B. Discrete-Time Observer Design

Once an appropriate continuous-time observer gain is determined, the discrete-time observer gain $\mathfrak{L}_d$ may be obtained using the same Caley-Tustin time discretization approach, as shown in (10).

$$\begin{aligned} \underline{\hat{x}}(\zeta,k) &= \mathfrak{A}_d \underline{\hat{x}}(\zeta,k-1) + \mathfrak{B}_d u(k) + \mathfrak{L}_d[y(k) - \hat{y}(k)] \\ \hat{y}(k) &= \mathfrak{C}_{d,o} \underline{\hat{x}}(\zeta,k-1) + \mathfrak{D}_{d,o} u(k) + \mathfrak{M}_{d,o} y(k) \end{aligned} \tag{10}$$

with $\mathfrak{A}_d$ and $\mathfrak{B}_d$ defined in (7), and $\mathfrak{C}_{d,o}$, $\mathfrak{D}_{d,o}$, $\mathfrak{M}_{d,o}$, and $\mathfrak{L}_d$ are given in (11).

$$\begin{aligned} \mathfrak{C}_{d,o}(\cdot) &= \sqrt{2\alpha}\,[I + \mathfrak{C}(\alpha I - \mathfrak{A})\mathfrak{L}_c]^{-1}\,\mathfrak{CR}(\alpha,\mathfrak{A})(\cdot) \\ \mathfrak{D}_{d,o} &= [I + \mathfrak{C}(\alpha I - \mathfrak{A})\mathfrak{L}_c]^{-1}\,\mathfrak{CR}(\alpha,\mathfrak{A})\mathfrak{B} \\ \mathfrak{M}_{d,o} &= [I + \mathfrak{C}(\alpha I - \mathfrak{A})\mathfrak{L}_c]^{-1}\,\mathfrak{CR}(\alpha,\mathfrak{A})\mathfrak{L}_c \\ \mathfrak{L}_d &= \sqrt{2\alpha}\mathfrak{R}(\alpha,\mathfrak{A})\mathfrak{L}_c \end{aligned} \tag{11}$$

It can been shown that using this approach, the discrete-time error dynamics will be stable if the continuous-time observer gain $\mathfrak{L}_c$ is chosen such that $\mathfrak{A}_o$ is stable. It is also worth noting that the proposed methodology skips the need for model reduction associated with the discrete-time Luenberger observer, with no spatial approximation required as well [9]–[13].

V. Model Predictive Controller Design

In this section, the observer-based MPC shown in Fig. 4 is developed with the goal of stabilizing the given unstable infinite-dimensional system within an optimal framework, relying solely on output measurements while satisfying input constraints. An infinite-time open-loop objective function sets the foundation of the controller design in the discrete-time setting at each sampling instant k. The objective function consists of a weighted sum of actuation costs as well as state deviations, for all future time instances, subject to the system dynamics and input constraints. Since full-state is assumed to be unavailable, reconstructed states are used to estimate states of the system, as shown in (12).

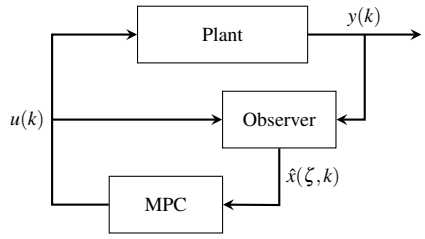

Fig. 4. Block diagram representation of the observer-based MPC.

$$\begin{aligned} \min_{U} \quad & \sum_{l=0}^{\infty} \langle \underline{\hat{x}}(\zeta,k+l|k), \mathfrak{Q}\underline{\hat{x}}(\zeta,k+l|k)\rangle \\ & + \langle u(k+l+1|k), \mathfrak{F}u(k+l+1|k)\rangle \\ \text{s.t.} \quad & \underline{\hat{x}}(\zeta,k+l|k) = \mathfrak{A}_d \underline{\hat{x}}(\zeta,k+l-1|k) + \mathfrak{B}_d u(k+l|k) \\ & u^{min} \le u(k+l|k) \le u^{max} \end{aligned} \tag{12}$$

where $\mathfrak{Q}$ and $\mathfrak{F}$ are positive definite operators of appropriate dimensions, responsible for penalizing state deviations and actuation costs, respectively. The notation $(k+l|k)$ indicates the future time states or input instance $k+l$ obtained at time k. The infinite-time optimization problem may be reduced to a finite-time setup by assigning zero-input beyond a certain control horizon N, resulting in the optimization problem in (13).

$$\begin{aligned} \min_{U} \quad & \sum_{l=0}^{N-1} \langle \underline{\hat{x}}(\zeta,k+l|k), \mathfrak{Q}\underline{\hat{x}}(\zeta,k+l|k)\rangle \\ & + \langle u(k+l+1|k), \mathfrak{F}u(k+l+1|k)\rangle \\ & + \langle \underline{\hat{x}}(\zeta,k+N|k), \mathfrak{P}\underline{\hat{x}}(\zeta,k+N|k)\rangle \\ \text{s.t.} \quad & \underline{\hat{x}}(\zeta,k+l|k) = \mathfrak{A}_d \underline{\hat{x}}(\zeta,k+l-1|k) + \mathfrak{B}_d u(k+l|k) \\ & u^{min} \le u(k+l|k) \le u^{max} \\ & \langle \underline{\hat{x}}(\zeta,k+N|k), \underline{\phi_u}(\zeta)\rangle = 0 \end{aligned} \tag{13}$$

Here, $\mathfrak{P}$ is the terminal cost operator obtained as the solution to the discrete-time Lyapunov equation, as shown in (14). This operator can be shown to be positive definite only if the terminal state $\underline{\hat{x}}(\zeta,k+N|k)$ is in a stable subspace. Therefore, for the resulting quadratic optimization problem to be convex, an equality constraint is introduced to guarantee $\mathfrak{P}$ is positive definite. The terminal constraint is enforced by setting the projection of the terminal state onto the unstable subspace of the system to zero [9], [14], [22].

$$\mathfrak{P}(\cdot) = \sum_{m=0}^{\infty}\sum_{n=0}^{\infty} -\frac{\langle \underline{\phi_m}, \mathfrak{Q}\underline{\psi_n}\rangle}{\lambda_m + \overline{\lambda_n}} \langle (\cdot), \underline{\psi_n}\rangle \phi_m \tag{14}$$

Here, $\underline{\phi_u}(\zeta)$ is the set of unstable eigenfunctions of the system, for all eigenvalues where $\mathrm{Re}(\lambda_u) \ge 0$. In addition, $\underline{\phi_i}$ and $\underline{\psi_i}$ correspond to the i^{th} eigenfunction of the original and

adjoint system, respectively. This problem can be further manipulated into a standard format for quadratic programming (QP) solvers. Refer to Appendix C for derivation details and results.

VI. Results and Discussion

Numerical simulations for the open-loop system and the closed-loop system under the proposed MPC are presented in this section, with parameters chosen according to Table I. As the eigenvalue distribution obtained in Fig(2) suggests, the open-loop system is unstable due to the presence of an eigenvalue with positive real part. The zero-input response of the system is shown in Fig(5) where the initial condition for the reactor is set to $c(\zeta,0)=\sin^2(\pi\zeta)$. The recycle stream is assumed to be empty at the beginning of the simulation.

An infinite-dimensional MPC is designed and applied to the unstable system. The state deviation and actuation penalty terms are set as $\mathfrak{Q}=0.04I$ and $\mathfrak{F}=27$. The sampling time and the horizon length for the MPC are set to $\Delta t=20$ s and $N=9$, respectively. Lastly, the input constraints are assumed to be $0\leq u(t)\leq 0.15$. The closed-loop response of the system is shown in Fig(6) and the control input as well as the system output is shown in Fig(7). It may be confirmed that the MPC successfully stabilizes the unstable system while satisfying the input constraints.

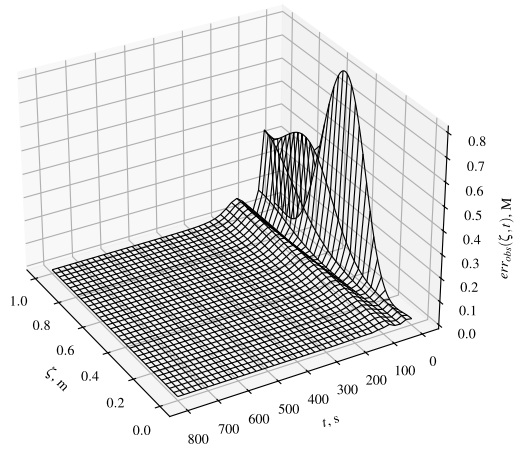

Fig. 5. Open-loop concentration profile along the reactor.

One interesting aspect of considering recycle stream is the oscillatory behavior of the system dynamics. While axial dispersion reactors show no oscillation in the absence of recycle, the nature of recycle streams can introduce such behavior. The choice of control horizon is another key factor. A short control horizon relative to the resident time of the recycle stream can lead to oscillatory input profiles due to the presence of delayed recycle stream. In this example, the control horizon, i.e. 180 s, is set to be considerably longer than the recycle delay, which is 80 s; resulting in a non-oscillatory input profile.

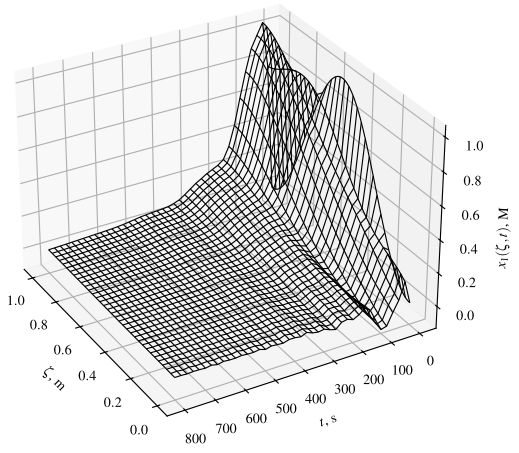

Fig. 6. Stabilized reactor concentration profile under the proposed MPC.

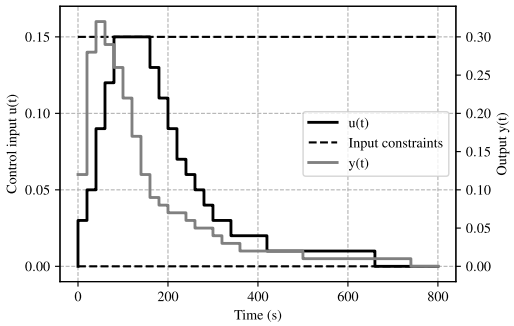

Fig. 7. Input constraints, the obtained input profile, and the reactor output under the proposed MPC.

Appendix

A. Adjoint System Operators

Utilizing the relation $\langle \mathfrak{A}\underline{x}+\mathfrak{B}u,\underline{y}\rangle=\langle \underline{x},\mathfrak{A}^*\underline{y}\rangle+\langle u,\mathfrak{B}^*\underline{y}\rangle$, the adjoint operators $\mathfrak{A}^*$ and $\mathfrak{B}^*$ are obtained in this part. The results are shown in (15) and (16) for $\mathfrak{A}^*$ and $\mathfrak{B}^*$, respectively.

$$\begin{aligned}\mathfrak{A}^* &= \begin{bmatrix} D\partial_{\zeta\zeta}+v\partial_\zeta+k_r & 0 \\ 0 & -\frac{1}{\tau}\partial_\zeta \end{bmatrix} \\ \mathscr{D}(\mathfrak{A}^*) &= \Big\{ \underline{y}=[y_1,y_2]^T\in Y : \\ &\qquad \underline{y}(\zeta),\partial_\zeta\underline{y}(\zeta),\partial_{\zeta\zeta}\underline{y}(\zeta) \quad \text{a.c.}, \\ &\qquad D\partial_\zeta y_1(1)+vy_1(1)=\frac{1}{\tau}y_2(1), \\ &\qquad Rvy_1(0)=\frac{1}{\tau}y_2(0), \partial_\zeta y_1(0)=0 \Big\}\end{aligned} \tag{15}$$

$$\mathfrak{B}^*(\cdot)=\begin{bmatrix} v(1-R)\int_0^1 \delta(\zeta)(\cdot)d\zeta & , & 0 \end{bmatrix} \tag{16}$$

Once the adjoint operators are determined, the eigenfunctions $\{\underline{\phi_i}(\zeta), \underline{\psi_i}(\zeta)\}$ (for $\mathfrak{A}$ and $\mathfrak{A}^*$, respectively) may be obtained and properly scaled following the calculation of eigenvalues. The system appears to be non-self-adjoint, as the obtained adjoint operator and its domain are not the same as the original operator and its domain. However, they share the same set of eigenvalues. Thus, the set of scaled eigenfunctions may be used to form a bi-orthonormal basis for the Hilbert space X; which will be later used in the controller design.

B. Resolvent Operator Derivation

One must obtain the resolvent operator of the system $\mathfrak{R}(s,\mathfrak{A}) = (sI-\mathfrak{A})^{-1}$ prior to constructing the discrete-time representation of the system. One way to obtain it is by utilizing the modal characteristics of the system, resulting in an infinite-sum representation of the operator. While being a common practice in the literature, truncating the infinite-sum representation for numerical implementation may lead to a loss of accuracy. Another way to express the resolvent operator is by treating it as an operator that maps either the initial condition of the system $\underline{x}(\zeta,0)$ or the input $u(t)$, to the Laplace transform of the state of the system $\underline{X}(\zeta,s)$. This approach, although more computationally intensive, results in a closed form expression for the resolvent operator, preserving the infinite-dimensional nature of the system. In (17), Laplace transform is applied to the LTI representation of the system for both zero-input response and zero-state response to obtain a general expression for the resolvent operator.

$$\begin{aligned}
&\dot{\underline{x}}(\zeta,t) = \mathfrak{A}\underline{x}(\zeta,t) + \mathfrak{B}u(t) \xrightarrow{\mathscr{L}} \\
&s\underline{X}(\zeta,s) - \underline{x}(\zeta,0) = \mathfrak{A}\underline{X}(\zeta,s) + \mathfrak{B}U(s) \\
&\begin{cases}
\xrightarrow{u=0} & \underline{X}(\zeta,s) = (sI-\mathfrak{A})^{-1}\underline{x}(\zeta,0) = \mathfrak{R}(s,\mathfrak{A})\underline{x}(\zeta,0) \\
\xrightarrow{\underline{x}(0,\zeta)} & \underline{X}(\zeta,s) = (sI-\mathfrak{A})^{-1}\mathfrak{B}U(s) = \mathfrak{R}(s,\mathfrak{A})\mathfrak{B}U(s)
\end{cases}
\end{aligned} \tag{17}$$

The goal is to obtain the solution for $\underline{X}(\zeta,s)$ and compare it with the general expression obtained in (17) to get the closed form expression for the resolvent operator. First step is to apply Laplace transform to the original system of PDEs in (4). The second order derivative term is decomposed to two first order PDEs, constructing a new 3×3 system of first order ODEs with respect to ζ after Laplace transformation, as shown in (18).

$$\begin{aligned}
\partial_\zeta \overbrace{\begin{bmatrix} X_1(\zeta,s) \\ \partial_\zeta X_1(\zeta,s) \\ X_2(\zeta,s) \end{bmatrix}}^{\tilde{\underline{X}}(\zeta,s)} &= \overbrace{\begin{bmatrix} 0 & 1 & 0 \\ \frac{s-k}{D} & \frac{v}{D} & 0 \\ 0 & 0 & s\tau \end{bmatrix}}^{P(s)} \begin{bmatrix} X_1(\zeta,s) \\ \partial_\zeta X_1(\zeta,s) \\ X_2(\zeta,s) \end{bmatrix} \\
&+ \underbrace{\begin{bmatrix} 0 \\ -\frac{x_1(\zeta,0)}{D} + v(1-R)\delta(\zeta)U(s) \\ -\tau x_2(\zeta,0) \end{bmatrix}}_{Z(\zeta,s)} \\
\Rightarrow \partial_\zeta \tilde{\underline{X}}(\zeta,s) &= P(s)\tilde{\underline{X}}(\zeta,s) + Z(\zeta,s)
\end{aligned} \tag{18}$$

with solution given by (19).

$$\tilde{\underline{X}}(\zeta,s) = \underbrace{e^{P(s)\zeta}}_{T(\zeta,s)}\tilde{\underline{X}}(0,s) + \int_0^\zeta \underbrace{e^{P(s)(\zeta-\eta)}}_{F(\zeta,\eta)} Z(\eta,s)d\eta \tag{19}$$

Since the boundary conditions are not homogeneous, $\tilde{\underline{X}}(0,s)$ needs to be obtained by solving the system of algebraic equations given in (20); which is the result of applying Danckwerts boundary conditions to the Laplace transformed system of PDEs at $\zeta = 1$.

$$\begin{aligned}
&\overbrace{\begin{bmatrix} -v & D & Rv \\ T_{11}(1,s) & T_{12}(1,s) & -T_{33}(1,s) \\ T_{21}(1,s) & T_{22}(1,s) & 0 \end{bmatrix}}^{M^{-1}(s)} \tilde{\underline{X}}(0,s) = \\
&\underbrace{\int_0^1 \begin{bmatrix} 0 \\ F_{33}(1,\eta)Z_3(\eta,s) - F_{12}(1,\eta)Z_2(\eta,s) \\ -F_{22}(1,\eta)Z_2(\eta,s) \end{bmatrix} d\eta}_{\underline{b}(s)} \\
&\Rightarrow \tilde{\underline{X}}(0,s) = M(s)\underline{b}(s)
\end{aligned} \tag{20}$$

Having access to $\tilde{\underline{X}}(0,s)$, the solution for $\underline{X}(\zeta,s)$ can be explicitly derived. The resolvent operator for zero-input and zero-state cases are therefore obtained in a closed form as shown in (21) and (22), respectively.

$$\begin{aligned}
&U(s) = 0 \Rightarrow \mathfrak{R}(s,\mathfrak{A})\underline{(\cdot)} = \begin{bmatrix} \mathfrak{R}_{11} & \mathfrak{R}_{12} \\ \mathfrak{R}_{21} & \mathfrak{R}_{22} \end{bmatrix} \begin{bmatrix} (\cdot)_1 \\ (\cdot)_2 \end{bmatrix} \Rightarrow \\
&\mathfrak{R}_{11} = \sum_{j=1}^{2} \frac{T_{1j}(\zeta)}{D} \int_0^1 \left[M_{j2}F_{12}(1,\eta) + M_{j3}F_{22}(1,\eta)\right](\cdot)_1 d\eta \\
&\qquad - \frac{1}{D}\int_0^\zeta F_{12}(\zeta,\eta)(\cdot)_1 d\eta \\
&\mathfrak{R}_{12} = \sum_{j=1}^{2} -\tau T_{1j}(\zeta) \int_0^1 M_{j2}F_{33}(1,\eta)(\cdot)_2 d\eta \\
&\mathfrak{R}_{21} = \frac{T_{33}(\zeta)}{D} \int_0^1 \left[M_{32}F_{12}(1,\eta) + M_{33}F_{22}(1,\eta)\right](\cdot)_1 d\eta \\
&\mathfrak{R}_{22} = -\tau T_{33}(\zeta) \int_0^1 M_{32}F_{33}(1,\eta)(\cdot)_2 d\eta \\
&\qquad - \tau \int_0^\zeta F_{33}(\zeta,\eta)(\cdot)_2 d\eta
\end{aligned} \tag{21}$$

$$\begin{aligned}
&\underline{x}(\zeta,0) = 0 \Rightarrow \mathfrak{R}(s,\mathfrak{A})\mathfrak{B}(\cdot) = \begin{bmatrix} \mathfrak{R}_1\mathfrak{B} \\ \mathfrak{R}_2\mathfrak{B} \end{bmatrix}(\cdot) \Rightarrow \\
&\mathfrak{R}_1\mathfrak{B} = -v(1-R)\big[\sum_{j=1}^{2} T_{1j}(\zeta)(M_{j2}T_{12}(1) + M_{j3}T_{22}(1)) \\
&\qquad - T_{12}(\zeta)\big](\cdot) \\
&\mathfrak{R}_2\mathfrak{B} = -v(1-R)\left[T_{33}(\zeta)(M_{32}T_{12}(1) + M_{33}T_{22}(1))\right](\cdot)
\end{aligned} \tag{22}$$

Since the system generator $\mathfrak{A}$ is not self-adjoint, the resolvent operator for the adjoint system shall also be obtained. This is done in a similar manner as the original system,

resulting in a closed-form expression for the adjoint resolvent operator $\mathfrak{R}^*(s,\mathfrak{A}^*)$. To avoid redundancy, the derivation of the resolvent operator for the adjoint system is not included in this manuscript.

C. Standard QP Representation for the MPC Optimization Problem

Simple algebraic manipulation can be done to utilize system dynamics in order to express future state estimations in terms of the current estimated state and a sequence of future inputs; transforming the optimization problem in (13) into the standard format accepted by conventional quadratic programming (QP) solvers, which is shown in (23).

$$
\begin{aligned}
&\min_{U} J = U^T\langle I,H\rangle U + 2U^T\langle I,P\underline{\hat{x}}(\zeta,k|k)\rangle \\
&\text{s.t.} \qquad U^{min} \le U \le U^{max} \\
&\qquad\quad T_u\underline{\hat{x}}(\zeta,k|k) + S_u U = 0 \\
&\text{with } H = \\
&\begin{bmatrix}
\mathfrak{B}_d^*\mathfrak{P}\mathfrak{B}_d+\mathfrak{F} & \mathfrak{B}_d^*\mathfrak{A}_d^*\mathfrak{P}\mathfrak{B}_d & \cdots & \mathfrak{B}_d^*{\mathfrak{A}_d^*}^{N-1}\mathfrak{P}\mathfrak{B}_d \\
\mathfrak{B}_d^*\mathfrak{P}\mathfrak{A}_d\mathfrak{B}_d & \mathfrak{B}_d^*\mathfrak{P}\mathfrak{B}_d+\mathfrak{F} & \cdots & \mathfrak{B}_d^*{\mathfrak{A}_d^*}^{N-2}\mathfrak{P}\mathfrak{B}_d \\
\vdots & \vdots & \ddots & \vdots \\
\mathfrak{B}_d^*\mathfrak{P}{\mathfrak{A}_d}^{N-1}\mathfrak{B}_d & \mathfrak{B}_d^*\mathfrak{P}{\mathfrak{A}_d}^{N-2}\mathfrak{B}_d & \cdots & \mathfrak{B}_d^*\mathfrak{P}\mathfrak{B}_d+\mathfrak{F}
\end{bmatrix} \\
&P = \begin{bmatrix}\mathfrak{B}_d^*\mathfrak{P}\mathfrak{A}_d & \mathfrak{B}_d^*\mathfrak{P}{\mathfrak{A}_d}^2 & \dots & \mathfrak{B}_d^*\mathfrak{P}{\mathfrak{A}_d}^N\end{bmatrix}^T \\
&T_u(\cdot) = \begin{bmatrix}\langle {\mathfrak{A}_d}^N(\cdot),\underline{\phi_u}\rangle\end{bmatrix} \\
&S_u = \begin{bmatrix}\langle {\mathfrak{A}_d}^{N-1}\mathfrak{B}_d,\underline{\phi_u}\rangle & \langle {\mathfrak{A}_d}^{N-2}\mathfrak{B}_d,\underline{\phi_u}\rangle & \dots & \langle \mathfrak{B}_d,\underline{\phi_u}\rangle\end{bmatrix} \\
&U = \begin{bmatrix}u(k+1|k) & u(k+2|k) & \dots & u(k+N|k)\end{bmatrix}^T
\end{aligned}
\tag{23}
$$

The optimal input sequence U is derived by solving the resulting QP problem at each sampling instant k. Following a receding horizon control strategy, only the first input of the optimal sequence, $u(k+1|k)$, is applied to the system to obtain the output measurement $y(k+1)$. Luenberger observer will then reconstruct the states at the sampling instant $k+1$ having access to the output and the input. This is followed by the optimization problem being solved again at the new sampling instant $k+1$, and the above strategy repeats itself.

REFERENCES

[1] W. H. Ray, *Advanced process control*. McGraw-Hill: New York, NY, USA, 1981.

[2] E. Davison, "The robust control of a servomechanism problem for linear time-invariant multivariable systems," *IEEE transactions on Automatic Control*, vol. 21, no. 1, pp. 25–34, 1976.

[3] A. A. Moghadam, I. Aksikas, S. Dubljevic, and J. F. Forbes, "Infinite-dimensional lq optimal control of a dimethyl ether (dme) catalytic distillation column," *Journal of Process Control*, vol. 22, no. 9, pp. 1655–1669, 2012.

[4] P. D. Christofides and P. Daoutidis, "Feedback control of hyperbolic pde systems," *AIChE Journal*, vol. 42, no. 11, pp. 3063–3086, 1996.

[5] M. Krstic and A. Smyshlyaev, "Backstepping boundary control for first-order hyperbolic pdes and application to systems with actuator and sensor delays," *Systems & Control Letters*, vol. 57, no. 9, pp. 750–758, 2008.

[6] X. Xu and S. Dubljevic, "The state feedback servo-regulator for countercurrent heat-exchanger system modelled by system of hyperbolic pdes," *European Journal of Control*, vol. 29, pp. 51–61, 2016.

[7] P. D. Christofides, "Robust control of parabolic pde systems," *Chemical Engineering Science*, vol. 53, no. 16, pp. 2949–2965, 1998.

[8] S. Dubljevic, N. H. El-Farra, P. Mhaskar, and P. D. Christofides, "Predictive control of parabolic pdes with state and control constraints," *International Journal of Robust and Nonlinear Control: IFAC-Affiliated Journal*, vol. 16, no. 16, pp. 749–772, 2006.

[9] S. Khatibi, G. O. Cassol, and S. Dubljevic, "Model predictive control of a non-isothermal axial dispersion tubular reactor with recycle," *Computers & Chemical Engineering*, vol. 145, p. 107159, 2021.

[10] D. Dochain, "State observers for tubular reactors with unknown kinetics," *Journal of process control*, vol. 10, no. 2-3, pp. 259–268, 2000.

[11] ——, "State observation and adaptive linearizing control for distributed parameter (bio) chemical reactors," *International Journal of Adaptive Control and Signal Processing*, vol. 15, no. 6, pp. 633–653, 2001.

[12] A. A. Alonso, I. G. Kevrekidis, J. R. Banga, and C. E. Frouzakis, "Optimal sensor location and reduced order observer design for distributed process systems," *Computers & chemical engineering*, vol. 28, no. 1-2, pp. 27–35, 2004.

[13] J. M. Ali, N. H. Hoang, M. A. Hussain, and D. Dochain, "Review and classification of recent observers applied in chemical process systems," *Computers & Chemical Engineering*, vol. 76, pp. 27–41, 2015.

[14] R. Curtain and H. Zwart, *Introduction to infinite-dimensional systems theory: a state-space approach*. Springer Nature, 2020, vol. 71, ch. 3.2: 'Riesz-spectral operators', pp. 79–108.

[15] M. Krstić, *Delay compensation for nonlinear, adaptive, and PDE systems*, ser. Systems & control. Birkhäuser, 2009, ch. 1.8: 'DDE or Transport PDE Representation', p. 9.

[16] S. Hiratsuka and A. Ichikawa, "Optimal control of systems with transportation lags," *IEEE Transactions on Automatic Control*, vol. 14, no. 3, pp. 237–247, 1969.

[17] L. Mohammadi, I. Aksikas, S. Dubljevic, and J. F. Forbes, "Lq-boundary control of a diffusion-convection-reaction system," *International Journal of Control*, vol. 85, no. 2, pp. 171–181, 2012.

[18] G. O. Cassol and S. Dubljevic, "Discrete output regulator design for a mono-tubular reactor with recycle," in *2019 American Control Conference (ACC)*, 2019, pp. 1262–1267.

[19] G. Ozorio Cassol, D. Ni, and S. Dubljevic, "Heat exchanger system boundary regulation," *AIChE Journal*, vol. 65, no. 8, p. e16623, 2019.

[20] J. Qi, S. Dubljevic, and W. Kong, "Output feedback compensation to state and measurement delays for a first-order hyperbolic pide with recycle," *Automatica*, vol. 128, p. 109565, 2021.

[21] V. Havu and J. Malinen, "The cayley transform as a time discretization scheme," *Numerical Functional Analysis and Optimization*, vol. 28, no. 7-8, pp. 825–851, 2007.

[22] Q. Xu and S. Dubljevic, "Linear model predictive control for transport-reaction processes," *AIChE Journal*, vol. 63, no. 7, pp. 2644–2659, 2017.

[23] O. Levenspiel, *Chemical reaction engineering*. John wiley & sons, 1998.

[24] K. F. Jensen and W. H. Ray, "The bifurcation behavior of tubular reactors," *Chemical Engineering Science*, vol. 37, no. 2, pp. 199–222, 1982.

[25] P. V. Danckwerts, "Continuous flow systems. distribution of residence times," *Chemical engineering science*, vol. 50, no. 24, pp. 3857–3866, 1993.

[26] E. Hairer, M. Hochbruck, A. Iserles, and C. Lubich, "Geometric numerical integration," *Oberwolfach Reports*, vol. 3, no. 1, pp. 805–882, 2006.